

# Melting and crystal structure of iron at high pressures and temperatures

Guoyin Shen<sup>1</sup>, Ho-kwang Mao, and Russell J. Hemley

Geophysical Laboratory and Center for High Pressure Research, Carnegie Institution of Washington, Washington DC

Thomas S. Duffy<sup>2</sup>, and Mark L. Rivers

Consortium for Advanced Radiation Sources, University of Chicago, Chicago, IL

**Abstract.** High-pressure melting, phase transitions and structures of iron have been studied to 84 GPa and 3500 K with an improved laser heated diamond anvil cell technique and *in situ* high P-T x-ray diffraction. At pressures below 60 GPa, the lower bound on the melting curve is close to those measured by *Boehler* [1993] and *Saxena et al.* [1993]; however, at pressures above 60 GPa our data indicate melting at higher temperatures than these studies, but still lower than the melting curve of *Williams et al.* [1990]. The  $\epsilon$ - $\gamma$ -l triple point is  $60(\pm 5)$  GPa and  $2800(\pm 200)$  K, based on our data of the  $\epsilon$ - $\gamma$  phase transition and the observation of melting by *in situ* x-ray diffraction. No solid phases other than  $\epsilon$ -Fe and  $\gamma$ -Fe were observed *in situ* at high temperatures ( $>1000$  K) and pressures to 84 GPa. However, the diffraction patterns of temperature quenched products at high pressure can be fit to other structures such as dhcp.

## Introduction

Our knowledge of the deep interior of the Earth is pieced together from information obtained from a number of measurements of physical and chemical properties of cosmochemically pertinent materials. Iron is thought to be the main constituent of the Earth's core because it is the most abundant element that satisfies the observed seismic velocities and densities. An accurate determination of its phase diagram and the equation of state at core conditions has been a long-sought goal of experimental geophysics. A number of experimental studies in the last few years have addressed the phase diagram of iron and its equation of state, but the increase in data has resulted in considerable confusion, particularly in regard to the phase diagram of iron. Unambiguous study requires *in situ* characterization of the sample's properties at well-defined pressure and temperature conditions.

In this paper, we report *in situ* x-ray diffraction measurements on iron at high P and T with the recently developed integrated technique of doubled sided multimode laser heated diamond anvil cell [Shen *et al.*, 1996]. X-ray diffraction was performed at the superconducting wiggler beamline X17B1 at the National Synchrotron Light Source (NSLS). The high pressure melting of iron was studied by *in situ* identification of solid and melt phases within a hot spot by x-ray diffraction. Phase relation and crystal structures were determined at pressures to 84 GPa and temperatures to 3500 K.

<sup>1</sup>Now at CARS, University of Chicago, Chicago.

<sup>2</sup>Now at Dept. of Geosciences, Princeton University, New Jersey.

Copyright 1998 by the American Geophysical Union.

Paper number 97GL03776.  
0094-8534/98/97GL-03776\$05.00

## Experimental Techniques

A double sided laser heating system [Shen *et al.*, 1996, Mao *et al.*, 1997] together with an energy dispersive diffractometer was set up at the X17B1 beamline. By introducing a multimode laser which has a flat-top power distribution with five times higher total power than the normally used TEMoo laser, temperatures of 1500 - 4000 K have been achieved with  $\pm 1$ -3% RMS variations and uniformity for 300 - 500 seconds in a sample disc of 20-50  $\mu$ m diameter [Shen *et al.*, 1996]. An imaging spectrometer allows us to monitor the temperature profiles at each measurement. A typical profile is given in Figure 1. The axial gradient is minimized by heating samples from both sides [Boehler *et al.* 1993; Mao *et al.* 1997; Shen *et al.* 1996].

The incident x-ray beam was controlled by a pair of adjustable slits and focused by a pair of grazing incidence Kirkpatrick-Baez (K-B) mirrors which are capable of focusing a 70  $\mu$ m incident white beam down to 3-5  $\mu$ m FWHM [Yang *et al.*, 1995]. The beam size at the sample position was measured by scanning a sharp edge [Mao and Hemley, 1996] and was set at  $10 \times 10$   $\mu$ m FWHM. By mounting diamond anvil cells on a rotary stage, the entire two dimensional diffraction cone can be collected and averaged. The rotation is especially useful for high-temperature studies where effects of recrystallization can be significant.

Two types of samples were used. One was pure iron powder ( $\sim 1$   $\mu$ m grain size), and the other was a mixture of iron and NaCl (or MgO, Al<sub>2</sub>O<sub>3</sub>) in a ratio of approximately 1:1 by volume. The mixture was used to avoid coarse crystal growth at high temperature [Funamori *et al.*, 1996]. One argument against using a mixture with oxides or halides is the possible reaction of iron with the medium [Boehler *et al.*, 1995]. In our study, no observable reactions were found by either x-ray diffraction or electron microprobe when materials were assured to be dry and loaded in

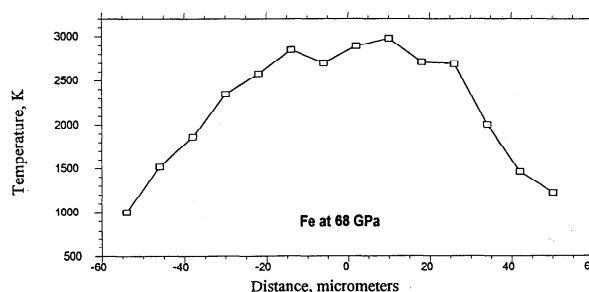


**Figure 1.** A typical temperature profile across the sample at 68 GPa with multimode laser heating. The collection time was 0.2 seconds. Any shorter period fluctuations in temperatures are therefore averaged out.

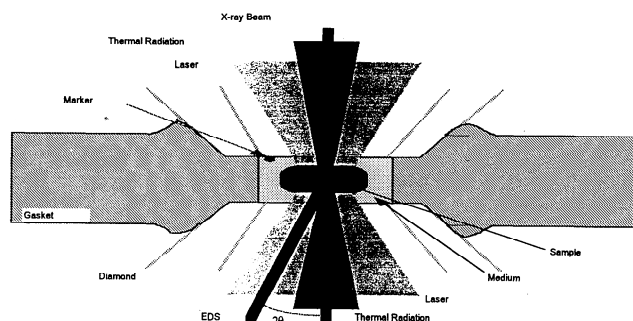


**Figure 2.** The sample geometry in a diamond anvil cell with double sided laser heating and *in situ* x-ray diffraction measurement.

inert conditions. NaCl, MgO, and  $\text{Al}_2\text{O}_3$  discs were used as media and isolation materials. These pressed polycrystalline discs were made between two diamond anvils to less than 5  $\mu\text{m}$  thickness. In addition of being chemically inert, a thermal insulator, and having low-strength, the preferred pressure media should have a simple x-ray diffraction pattern with peaks that do not overlap with those of iron. Among the tested materials, NaCl is considered to be the most suitable medium and  $\text{Al}_2\text{O}_3$  to be the least.

The sample geometry is shown schematically in Figure 2. A  $\sim 5 \mu\text{m}$  metallic chip of Au, Pt, or W was placed between the sample and the gasket, making the chip optically visible. The laser heating optics and the x-ray beam were then aligned to within 2  $\mu\text{m}$ . This was accomplished by first locating the chip at the x-ray beam position. The laser heating system was then aligned to the chip position.

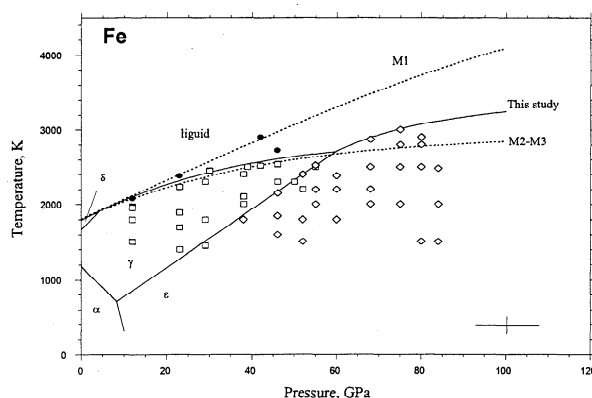
## High-Pressure Melting Of Iron

Figure 3 shows our results on high-pressure melting of iron based on *in situ* x-ray diffraction measurements. Pressures were determined by the equations of state of  $\epsilon$ -Fe [Mao *et al.*, 1990], MgO [Jamieson *et al.*, 1982] prior to laser heating. One question in pressure determination is the thermal pressure contribution at high temperature [e.g., Heinz, 1990, Fiquet *et al.*, 1996]. It is possible to measure thermal pressures by adding a standard with known P-V-T equation of state. Typically, from runs with a platinum metal with the same sample preparation procedure, the thermal pressure contribution is from 1 to 8 GPa at about 2000 K and at pressures similar to those in this study. Temperatures were measured spectroradiometrically [Shen *et al.*, 1996]. The main source of systematic error in the temperature estimate arises from the temperature gradient in a small hot spot. Therefore, a significant advantage in using a multimode laser with a flat-top intensity profile is to provide a uniform and large hot spot on the sample, yielding a more accurate temperature determination in laser heating experiments. A typical uncertainty in pressure and temperature is shown in Figure 3.

When crystalline peaks appear at a certain P-T condition, we assign that P-T point as solid, because the whole sampling volume is uniformly heated and the diameter of the heated volume (20 - 50  $\mu\text{m}$ ) is much larger than the x-ray beam size (10x10  $\mu\text{m}$ ). However, when there is a loss of diffraction peaks, it is not always certain whether the material has melted. While the small x-ray beam ensures the probing of a uniform high P-T region, the number of crystallites within the sampling region may be statistically insufficient for polycrystalline x-ray diffraction analysis.

Possible crystal growth at high temperatures further compounds the problem. Several procedures were employed to minimize this effect. First, the iron sample was mixed with MgO (or  $\text{Al}_2\text{O}_3$  or NaCl) powder in a ratio of approximately 1:1 by volume. Although the mixture sample helps to prevent the coarse crystallinity, we still often observe the preferred orientation effect at high temperature, i.e., odd peak intensities or even missing diffraction peaks. Furthermore, by rotating the diamond cell around its axis, the entire diffraction cone is collected and averaged. With the laser beam coaxial to the rotating axis, the heating spot is unaffected by the rotation. In addition, efforts were made during experiments to bracket the melting temperatures by increasing and decreasing temperatures to observe the loss of diffraction peaks and reappearance of crystalline peaks, respectively. Despite these efforts, we caution that the conclusive identification of melts is still limited by the EDXD technique. Further improvements in the use of x-ray diffraction for identifying melting should be possible with area detection techniques and by direct measurement of the structure factor of the melt.

Representative diffraction patterns are shown in Figure 4. In Figure 4a, iron crystallizes in hexagonal-close-packed (hcp)  $\epsilon$  structure at 23 GPa at ambient temperature. As the temperature was raised to  $1861 \pm 50$  K, the hcp diffraction peaks disappeared completely, and new peaks corresponding to the face-centered-cubic (fcc)  $\gamma$  structure appeared. The diffraction peaks of  $\gamma$  iron disappeared above  $2378 \pm 50$  K and reappeared when temperature was lowered to  $2220 \pm 50$  K, bracketing the melting temperature. The completeness of the transition is a clear indication that the entire region sampled by the x-ray diffraction has uniform P-T conditions, a major improvement relative to previous experiments [e.g., Saxena *et al.*, 1995; Yoo *et al.*, 1995]. The clear thermal shift of diffraction peaks shows that the laser heating spot and the x-ray beam are well aligned and the alignment is maintained as temperature increases. In Figure 4b, iron crystallizes in hcp  $\epsilon$  structure at 68 GPa at ambient temperature. The hcp diffraction peaks are preserved until the temperature was raised above



**Figure 3.** Phase diagram of iron based on the *in situ* high P-T x-ray diffraction measurements. M1 - Williams *et al.* [1991]; M2 - Boehler *et al.* [1990], Boehler [1993]; M3 - Shen *et al.* [1993], Saxena *et al.* [1993]. The shock wave data are not shown for clarity. Solid circles denote melts and they are shown only when we were able to bracket the melting temperature by cycling the temperature above and below the melting curve. Otherwise, only the corresponding crystalline phases are shown, with their highest temperature representing the lower bound of the melting curve. Open squares are  $\gamma$ -Fe and open diamonds are  $\epsilon$ -Fe. A typical error bar is shown at the lower-right corner.

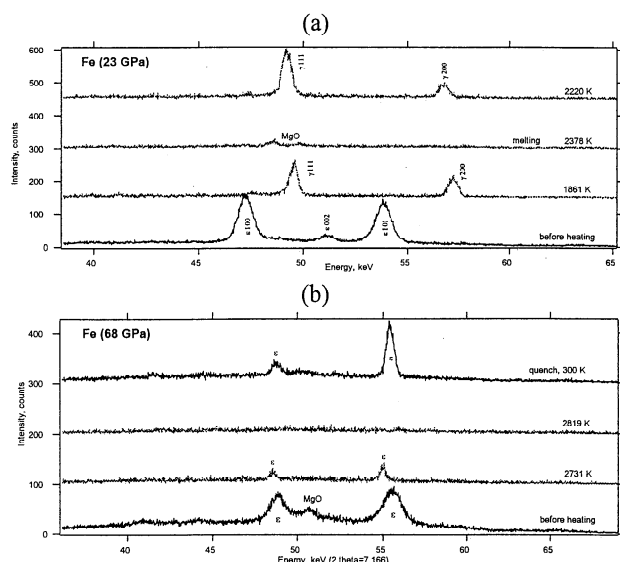


**Figure 4.** Diffraction spectra measured at in situ high P-T conditions. **a:** iron at 23 GPa. In this run we were able to bracket the melting by cycling temperatures around the melting curve. **b:** iron at 68 GPa. The highest temperature of the observed crystalline diffraction represents the lower bound of the melting curve. The diffraction collection time is typically 10 - 30 seconds at high temperatures.

2819±150 K, where there was a loss of diffraction peaks. When the temperature was lowered to 2520±150 K, still no diffraction peaks were observed, preventing conclusively bracketing the melting temperature. In this case, experiments were repeated at similar pressures, and efforts were made to observe the highest temperature before the loss of crystalline peaks. These data, therefore, represent a lower bound to the melting curve.

In Figure 3, the melts are shown only when we were able to bracket the melting temperature by cycling the temperature around melting curve. Otherwise, only the corresponding crystalline phases are shown, with their highest temperature representing the lower bound of the melting curve. Two runs at the highest pressures in this study were aimed at studying the recently reported double hcp phase [Saxena *et al.*, 1995; Yoo *et al.*, 1995] (see below), and the highest temperature may not reflect iron melting. The solid line in Figure 3 represents the lower bound on the melting curve. At pressures below 60 GPa, our line is close to M2-M3 curve, which implies that the M2-M3 curve is a lower bound on the iron melting curve in this pressure range, a result consistent with the recent study of Jephcoat and Besedin [1996]. Above 60 GPa, our data show that there is an increase in melting slope ( $dT/dP$ ) and our lower bound to the melting curve is higher in temperature than M2-M3 and lies between M2-M3 and M1. The slope increase qualitatively agrees with Boehler [1993], but our data show that it happens at lower pressures (60 GPa). This is consistent with the triple point ( $\epsilon$ - $\gamma$ -I) location based on our data for the solid-solid phase transition. Due to limited points and uncertainties in identification of the melt at pressures above 60 GPa, it is difficult to quantitatively extrapolate the melting to core pressures.

In comparing our results with previously reported data, it is worth discussing the criteria used to identify melting. Jeanloz and Kavner [1996] summarized five types of melting criteria, namely fluid flow, glass feature, quench texture, change in sample properties, and temperature versus laser power correlation.

They concluded that the most reliable criteria for determining melting inside the laser heated diamond cell are fluid flow and quenched glass observations. The criterion of textural change (fluid flow) has been adopted by Boehler [1993], Jephcoat and Besedin [1996] and Sitaud and Thevenin [1996]. However, the underlying cause of the textural change is still not well established. Shen *et al.* [1993] pointed out that the textural change becomes less obvious as pressure increases; above 40 GPa, only very occasional and small movement is typically observed, making it difficult to identify the onset of melting. We believe that x-ray diffraction provides a more reliable way to recognize melting. However, preferred orientation and coarse crystallinity at high temperature make it difficult to recognize melting with EDXD technique. As shown in Figure 3, most runs only gives us the highest temperatures where solid crystalline phases were observed. These values could be close to the melting temperatures since experiments were repeated several times in a similar pressure range, and we tried to minimize the coarse crystallinity and to increase the statistics for x-ray diffraction analysis as mentioned previously. As a result, we consider these data to be a lower bound on the melting curve. Further technical improvements may include using area detectors to further increase statistics or observing the positive signals such as the structure factor of melt.

### High P-T Phases

A line is drawn in Figure 3 to represent the  $\epsilon$ - $\gamma$  phase boundary based on our x-ray diffraction data and the  $\alpha$ - $\gamma$ - $\epsilon$  triple point of Akimoto *et al.* [1987]. The phase transition is recognized by the appearance of the  $\gamma$  phase with increasing temperature. The volume difference between  $\epsilon$  and  $\gamma$  is found to be 0.5-2% at the phase boundary. The phase boundary of this study is consistent with Mao *et al.* [1987], but is at slightly higher temperatures than those of Boehler [1986] and the three points determined by Fumamori *et al.* [1996]. The present P-T range covers the entire stability field of the  $\gamma$  phase, which allows us to better constrain the phase relations up to the melting curve and, thus, the location of the  $\epsilon$ - $\gamma$ -I triple point. Boehler [1993] made the measurements of the  $\epsilon$ - $\gamma$  transition to over 70 GPa based on an indirect visual observation of small changes of optical absorption and/or changes in the slope of the laser power/temperature function. His data do not agree with the present study. We conducted several runs at pressures above 60 GPa and temperatures to 3000 K, and no  $\gamma$ -Fe was observed in these runs. This deviation leads to different locations of the  $\epsilon$ - $\gamma$ -I triple point with 60±5 GPa-2800±200 K from our data versus 100 GPa-2900 K from Boehler [1993]. The present location of the triple point is close to those of Boehler [1986] (75 GPa-2500 K) with the resistance heating method, Saxena *et al.* [1993] (65 GPa-2700 K) with laser heating, and Yoo *et al.* [1995] (50 GPa-2500 K) with a combined x-ray diffraction and single-sided laser heating technique.

Saxena *et al.* [1995] found that laser heated iron (quenched from high temperature) at 30 to 40 GPa transformed to a dhcp structure. The stability range of the structure was further extended to 60 GPa by Saxena *et al.* [1996] on temperature-quenched run products. Yoo *et al.* [1996] observed the dhcp structure at pressures below 40 GPa by in situ x-ray diffraction at high temperature with single sided laser heating. Very recently, Andrault *et al.* [1997] found the orthorhombic structure of iron at high P-T. In this study, no new phases other than  $\epsilon$  and  $\gamma$  at pressures above 12 GPa and temperatures above 1400 K were observed. However, we do observe dhcp structure on temperature quenched products while samples are at high pressures (<60

GPa). In the previous studies by Saxena *et al.* [1995] and Yoo *et al.* [1995], a low power TEM<sub>00</sub> YAG laser was used and the sample was heated only from one side. This technique inevitably leads to strong temperature gradients both in radial and axial directions, resulting in x-ray diffraction from a sample at various temperatures. For example, from their reported diffraction patterns, a mixture of diffraction with  $\epsilon$ -Fe and  $\gamma$ -Fe can often be seen. In contrast, our improved system records the diffraction data from well-defined P-T conditions. As shown in Figure 4, a complete transition from  $\epsilon$  phase to  $\gamma$  phase can be clearly observed at high temperature, indicating that the entire sampled region for x-ray diffraction has uniform P-T. So we conclude that the appearance of the dhcp structure is an effect of the temperature gradient in these earlier experiments. In other words, the dhcp peaks observed in situ probably arise from regions of the sample at very low temperatures and the resulting incomplete transformation between  $\epsilon$  and  $\gamma$ . The observation of the dhcp structure of Saxena *et al.* [1995] was based on the temperature quenched runs and thus does not conflict with our observations. However, Saxena *et al.* [1995] proposed a stability field for the  $\beta$ -phase at high P-T. This study shows that the appearance of the dhcp structure as a temperature-quench product (or the result of incomplete transformation) indicates that the phases ( $\epsilon'$  or  $\beta$ ) have no stability field, at least in the indicated P-T range. The alignment of the x-ray beam and the laser heating spot is often not described in detail in the reported studies and its importance is usually ignored in explaining the x-ray diffraction from laser heated diamond cells. As mentioned previously, we align the laser spots and the x-ray beam to the same point (2  $\mu$ m accuracy) by comparing and coordinating the two dimensional x-ray image and the optical microscope images. We check the completeness of the phase transition (e.g.,  $\epsilon$ -Fe to  $\gamma$ -Fe, Figure 4a) and the sign of thermal shift of diffraction peaks as temperature increases to make sure proper alignment and that it is maintained as the experiment continues. Good alignment and well-defined P-T conditions are essential for obtaining unambiguous information.

**Acknowledgement.** Thanks are due to Drs. Jingzhu Hu, Viktor Struzhkin, Ren Lu, Yan-zhang Ma, and Dion Heinz for help during the experiments at X17B, National Synchrotron Light Source. Comments by two anonymous reviewers improved the manuscript. This work was funded by NSF and W.M. Keck Foundation.

## References

- Akimoto, S., T. Suzuki, T. Yagi, O. Shimomura, Phase diagram of iron determined by high pressure/temperature x-ray diffraction using synchrotron radiation, in *High Pressure Research in Mineral Physics*, edited by M. H. Manghnani and Y. Syono, Terr/AGU, 149-154, 1987.
- Andrault, D., G. Fiquet, M. Kunz, F. Visocekas, D. Hausermann, The orthorhombic structure of iron: An in situ study at high-temperature and high pressure, *Science*, 278, 831-834, 1997.
- Boehler, R., The phase diagram of iron to 430 kbar, *Geophys. Res. Lett.*, 13, 1153-1156, 1986.
- Boehler, R., Temperatures in the Earth's core from melting-point measurements of iron at high static pressures, *Nature*, 363, 534-536, 1993.
- Boehler, R., N. Von Bargen and A. Chopelas, Melting, thermal expansion, and phase transitions of iron at high pressures, *J. Geophys. Res.*, 95, 21,731-21,736, 1990.
- Boehler, R., G. Fiquet, H.-J. Reichmann, A. Zerr, New laser heating technique at high pressure, high temperature: Equation of state of Mo and Fe, Abstract, *HASYLAB*, 649, 1993.
- Boehler, R., A. Chopelas, and A. Zerr, Temperature and chemistry of the core-mantle boundary, *Chem. Geology*, 120, 199-205, 1995.
- Fiquet, G., D. Andrault, J. P. Itie, P. Gillet, and P. Richet, High pressure and high temperature x-ray diffraction study of periclase in a laser heated diamond anvil cell, *Phys. Earth Planet. Int.*, 95, 1-17, 1996.
- Funamori, N., T. Yagi, and T. Uchida, High-pressure and high temperature in situ x-ray diffraction study of iron to above 30 GPa using MA8-type apparatus, *Geophys. Res. Lett.*, 23, 953-956, 1996.
- Heinz, D. L., Thermal Pressure in the laser heated diamond anvil cell, *Geophys. Res. Lett.*, 17, 1161-1164, 1990.
- Jamieson, J.C., J.N. Fritz, and M.H. Manghnani, Pressure measurement of high temperatures in x-ray diffraction studies: Gold as a primary standard, in *High Pressure Research in Geophysics*, edited by S. Akimoto and M. H. Manghnani, Tokyo: Center for Academic Publishing, 27-48, 1982.
- Jeanloz, R. and A. Kavner, Melting criteria and imaging spectroradiometry in laser heated diamond-cell experiments, *Phil. Trans. R. Soc. Lond. A*, 354, 1279-1305, 1996.
- Jephcoat, A. P., and S. P. Besedin, Temperature measurement and melting determination in the laser-heated diamond cell, *Phil. Trans. R. Soc. Lond. A*, 354, 1333-1360, 1996.
- Mao, H. K. and R. J. Hemley, Energy dispersive x-ray diffraction of micro-crystal at ultrahigh pressures, *High Pressure Research*, 14, 257-267, 1996.
- Mao, H. K., P. M. Bell, and C. Hadidiacos, Experimental phase relations of iron to 360 kbar and 1400 C, determined in an internally heated diamond anvil apparatus, in *High Pressure Research in Mineral Physics*, edited by M. H. Manghnani and Y. Syono, Terr/AGU, 135-138, 1987.
- Mao, H. K., Y. Wu, L. C. Chen, J. F. Shu, A. P. Jephcoat, Static compression of iron to 300 GPa and Fe<sub>0.8</sub>Ni<sub>0.2</sub> alloy to 260 GPa: implications for composition of the core, *J. Geophys. Res.*, 95, 21,737-21,742, 1990.
- Mao, H. K., G. Shen, R. J. Hemley, and T. S. Duffy, X-ray diffraction with a double hot plate laser heated diamond cell, *High Pressure Temperature Research: Properties of Earth and Planetary Materials*, in press, 1997.
- Saxena, S. K., G. Shen, and P. Lazor, Experimental evidence for a new iron phase and implications for Earth's core, *Science*, 260, 1312-1314, 1993.
- Saxena, S. K., L. S. Dubrovinsky, P. Haggkvist, Y. Cerenius, G. Shen and H. K. Mao, Synchrotron x-ray study of iron at high pressure and temperature, *Science*, 269, 1703-1704, 1995.
- Shen, G., P. Lazor, S. K. Saxena, Melting of wustite and iron up to pressures of 600 kbar, *Phys. Chem. Minerals*, 20, 91-96, 1993.
- Shen, G., H. K. Mao and R. J. Hemley, Laser-heating diamond-anvil cell technique: Double-sided heating with multimode Nd:YAG laser, *Advanced Materials '96 - New Trends in High Pressure Research*, Proc. 3<sup>rd</sup> NIRIM ISAM, pp. 149-152, Tsukuba, Japan, 1996.
- Williams, Q., E. Knittle, and R. Jeanloz, The high pressure melting curve of iron: A technical discussion, *J. Geophys. Res.*, 96, 2171-2184, 1991.
- Yang, B. X., M. Rivers, W. Schildkamp and P. J. Eng, GeoCARS micro-focusing Kirkpatrick-Baez mirror bender development, *Rev. Sci. Instrum.*, 66, 2278-2280, 1995.
- Yoo, C. S., J. Akella, A. Compbell, H. K. Mao, and R. J. Hemley, Phase diagram of iron by in situ X-ray diffraction: implications for the Earth's core, *Science*, 270, 1473-1475, 1995.

R.J. Hemley, H.K. Mao, G. Shen, Geophysical Laboratory and Center of High Pressure Research, Carnegie Institution of Washington, 5251 Broad Branch Road, Washington DC, 20015.

T.S. Duffy, M.L. Rivers, CARS, University of Chicago, 5640 South Ellis Avenue, Chicago, IL 60637.

(Received August 27, 1997; revised November 25, 1997; accepted December 16, 1997)